

Thermally and Mechanically Enhanced Epoxy Resin-Silica Hybrid Materials Containing Primary Amine-Modified Silica Nanoparticles

Kung-Chin Chang,¹ Chang-Yu Lin,¹ Hui-Fen Lin,¹ Sheng-Che Chiou,¹ Wan-Chun Huang,¹ Jui-Ming Yeh,¹ Jen-Chang Yang²

¹Department of Chemistry, Center for Nanotechnology at CYCU and R & D Center for Membrane Technology, Chung-Yuan Christian University, Chung Li 32023, Taiwan, Republic of China

²Department of Organic Chemistry, Chemical Systems Research Division, Chung-Shan Institute of Science & Technology, Lung-Tan 325, Taiwan, Republic of China

Received 26 March 2007; accepted 26 August 2007

DOI 10.1002/app.27559

Published online 29 January 2008 in Wiley InterScience (www.interscience.wiley.com).

ABSTRACT: In this article, a series of hybrid materials consisted of epoxy resin matrix and well-dispersed amino-modified silica (denoted by AMS) nanoparticles were successfully prepared. First of all, the AMS nanoparticles were synthesized by performing the conventional acid-catalyzed sol-gel reactions of tetraethyl orthosilicate (TEOS), which acts as acceded sol-gel precursor in the presence of 3-aminopropyl trimethoxysilane (APTES), a silane coupling agent molecules. The as-prepared AMS nanoparticles were then characterized by FTIR, ¹³C-NMR, and ²⁹Si-NMR spectroscopy. Subsequently, a series of hybrid materials were prepared by performing *in situ* thermal ring-opening polymerization reactions of epoxy resin in the presence of as-prepared AMS nanoparticles and raw silica (RS) particles (i.e., pristine silica). AMS nanoparticles were found

to show better dispersion capability in the polymer matrices than that of RS particles based on the morphological observation of transmission electron microscopy (TEM) study. The better dispersion capability of AMS nanoparticles in hybrid materials was found to lead enhanced thermal, mechanical properties, reduced moisture absorption, and gas permeability based on the measurements of thermo gravimetric analysis (TGA), differential scanning calorimetry (DSC), dynamic mechanical analysis (DMA), and gas permeability analysis (GPA), respectively. © 2008 Wiley Periodicals, Inc. *J Appl Polym Sci* 108: 1629–1635, 2008

Key words: resins; silicas; amine-modified silica; thermal properties; mechanical properties

INTRODUCTION

Organic-inorganic hybrid (or nanocomposite) materials have evoked intensive and extensive academic and industrial research activities in the recent decade due to their unique properties resulted from the integration of the characteristics of organic and inorganic component at the molecular level. The ultimate physical properties of nanocomposites depend strongly on the particle size, shape, degree of dispersed particles, and the interactions occurred between the interface of particles and polymer matrix.^{1,2} However, when the dimension of inorganic additives reduced to nanoscale size,^{3,4} the difficulty of homogeneously dispersing inorganic parts in the organic matrix is

dramatically increased, owing to the lack of affinity between the interfacial contact area of inorganic fillers and organic polymers. Therefore, finding remedial measures for this flaw are important for the development of new nanocomposites. The surface modification (or functionalization) of inorganic fillers by an organic agent (modified agent) was usually an effective way to enhance compatibility between two phases.

Epoxy resin nanocomposites are used popularly in a variety of industrial applications because of their unique physical properties,^{5–15} such as thermal stability, mechanical strength, dimensional stability, low density, chemical resistance, flame retardant, and electrical resistant can be varied considerably. Recently, Sun and coworkers¹⁶ compared the effects of nanosized and microsized fillers in epoxy composites by means of differential scanning calorimetry and thermomechanical measurements, indicating that the glass transition temperature was reduced as the amount of nanofillers increased whereas it did not change in the corresponding microcomposites. Contrasting effects have also been reported in other works for different fillers in various matrices where

Correspondence to: J.-M. Yeh (juiming@cycu.edu.tw).

Contract grant sponsor: NSC; contract grant number: 95-2627-M-033-001.

Contract grant sponsor: Center-of-Excellence Program on Membrane Technology, the Ministry of Education, Taiwan, Republic of China.

both an increase¹⁷ and a decrease¹⁸ of the thermomechanical properties were reported and sometimes even more complicated nonmonotonic trends were observed with the best performance at low filler-level as 5% by weight.¹⁹

In our earlier research work, the surface organo-modification of nanolayered clay platelets was done by performing cationic exchange reactions between the sodium ions existed in the interlayer regions of Na⁺-montmorillonite (MMT) clay and the various cationic surfactants.²⁰ The organo-modified MMT had been found to show a well-dispersed capability in polymer matrix than that of raw MMT, leading to effective enhancement of physical properties of polymers. However, a report associated with the effect of organo-modified silica nanoparticles on physical properties of polymers has relatively seldom been mentioned.

Therefore, in this study, we present a series of study on the effect of primary amine-modified silica nanoparticles on the physical properties of as-prepared hybrid materials. First of all, we synthesized the AMS nanoparticles by carrying out the conventional acid-catalyzed sol-gel reactions of TEOS in the presence of APTES molecules. The as-prepared particles were then characterized by FTIR, ¹³C-NMR, and ²⁹Si-NMR spectroscopy. Subsequently, a series of hybrid materials were prepared by performing *in situ* thermal ring-opening polymerization reactions of epoxy resin in the presence of as-prepared AMS nanoparticles and RS particles separately. TEM measurement shows that the dispersion of AMS nanoparticles in the epoxy polymer matrices is better than that of RS particles which lead to more effective enhancement of thermal, mechanical properties, and reduced gas permeability based on the measurements of TGA, DSC, DMA, and GPA, respectively.

EXPERIMENTAL

Chemicals and instruments

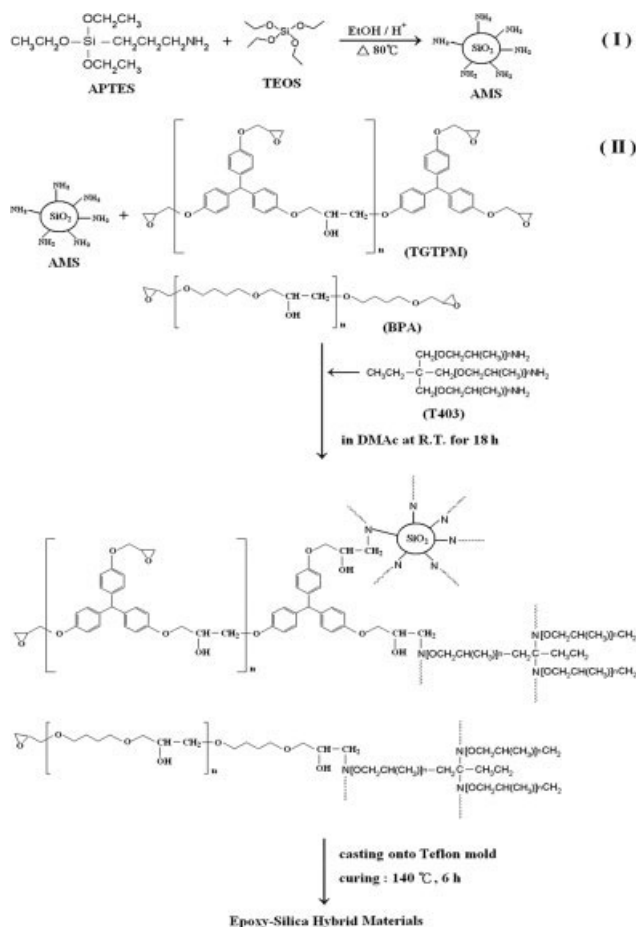
The epoxy resin used in this study was triphenylol-methane triglycidyl ether (TGTPM; Aldrich) and 1,4-Butanediol diglycidyl ether (BPA; Aldrich, 95.0%). The hardener was trimethylolpropane tris[poly(propylene glycol), amine terminated] ether (T-403; Aldrich). Tetraethyl orthosilicate (TEOS; Fluka, 98.0%) and (3-Aminopropyl)trimethoxysilane (APTES; Fluka, 98.0%) were used as sol-gel precursor and silane coupling agent, respectively. Ethanol (EtOH; Riedel-de Haën, 99.8%), Hydrochloric acid (HCl; Riedel-de Haën, 37.0%), and *N,N*-Dimethylacetamide (DMAc; 99.0%, Riedel-de Haën) were used as received without further purification.

Fourier Transformation Infrared (FTIR) spectra were obtained at a resolution of 4.0 cm⁻¹ with a

FTIR (BIO-RAD FTS-7, Philadelphia, USA) spectrophotometer at room temperature ranging from 4000 to 400 cm⁻¹. Both ¹³C and ²⁹Si MAS solid-state NMR experiments were performed on a 400 MHz chemagnetics solid-state NMR spectrometer. ¹³C MAS NMR spectra were obtained at 100.63 MHz with 7 kHz applying 90° pulses and 2.0 s pulse delays. To enhance carbon sensitivity, cross-polarization (CP) techniques were employed. ²⁹Si MAS NMR spectra were recorded at 79.49 MHz applying 90° pulses, 300 s pulse delays, and 5.0 ms contact time, with samples in 5.0 mm zirconia rotors spinning at 7 kHz. The samples for TEM study were first prepared by the membrane of hybrid materials being placed into epoxy resin capsules, and this was followed by the curing of the epoxy resin at 100°C for 24 h in a vacuum oven. The cured epoxy resin containing hybrid materials was microtomed with a Reichert-Jung Ultracut-E (Switzerland) into 60- to 90-nm thick slices. Subsequently, one layer of carbon about 10-nm thick was deposited on these slices on 300-mesh copper nets for TEM observations on a JEOL-200FX (Tokyo, Japan) with an acceleration voltage of 120 kV. TGA and DSC were employed to record the thermal stability of specimens. TGA scans were performed on a DuPont TA Q50 (New York, USA) thermal analysis system in air atmosphere. The scan rate was 20°C/min, and temperature range was from 35 to 800°C. DSC was performed on a DuPont TA Q10 (New York, USA) differential scanning calorimeter at a heating or cooling rate of 10°C/min in nitrogen atmosphere. The temperature range was from 0 to 100°C. The DMA of the hybrid materials were performed from 30 to 100°C with a DuPont TAQ800 (New York, USA) analyzer at a heating rate of 3°C/min and at a frequency of 1 Hz. A Yanagimoto Co., Ltd. Gas permeability analyzer (model GTR 10, Japan) was employed to perform the permeation experiment of oxygen/nitrogen gas. The unit of gas permeability was "Barrer" (1 Barrer = 10⁻¹⁰ cm³STP cm/cmHg s cm²).²¹ The immersion weight gains (wt %) of the pure epoxy and hybrid materials were calculated after 24 h of water uptake periods at room temperature.²⁰

Synthesis of AMS nanoparticles

The AMS nanoparticles were prepared by conventional acid-catalyzed sol-gel reactions of TEOS in the presence of APTES molecules, as shown in Scheme 1 (I). A typical procedure to prepare the AMS nanoparticles was given as follows: 18.75 g (0.09 mole) of TEOS, 7.2 g of 1N HCl, and 10.0 g of EtOH in a 250-mL of three-neck round-bottom flask connected with a condenser, a thermometer, and nitrogen gas inlet/outlet. Nitrogen gas was bubbled into the flask throughout the reaction. Under the magnetic stirring,



Scheme 1 Preparation of AMS nanoparticles and epoxy-silica hybrid materials.

the solution was heated to 80°C and maintained for 3 h. A separate solution containing 2.21 g (0.01 mole) of APTES and 10.0 g of 1N HCl are magnetically stirred for 3 h at room temperature. Subsequently, the APTES solution was added into the TEOS gel solution with stirring for 30 min at room temperature. The solvents from the sol-gel reactions were allowed to evaporate under the fume hood for 72 h. The AMS nanoparticles were thus obtained. The RS particles were also prepared as control experiments without the addition of APTES monomers.

Preparation of epoxy-silica hybrid materials

The typical procedure to prepare the epoxy-silica hybrid (nanocomposite) materials was shown in Scheme 1 (II). Using this approach, 0.5 g of TGTPM and 0.5 g of BPA were dissolved in 12 g of DMAC under stirring for 6 h. The AMS nanoparticles or RS particles as mentioned above in various feeding composition of 0, 3, and 5 wt % of silica was introduced. Subsequently, 0.68 g of T-403 functioned as curing agent was added and stirred magnetically for 12 h at room temperature. The resultant mixture was degassed and cast drop-wisely onto a clean Teflon mould followed by curing at 140°C for 6 h. The cured hybrid films were obtained with a thickness of about 170 μm.

RESULTS AND DISCUSSION

The preparation of AMS nanoparticles and RS particles was carried out by performing the conventional acid-catalyzed sol-gel reactions of TEOS with/without the addition of APTES. For the introduction of 5 wt % AMS nanoparticles in epoxy resin matrix (e.g., AMS5), the actual chemical reactions involved was probably associated with the formation of chemical bonding resulted from the thermal epoxide ring-opening polymerization reactions occurred between the epoxide ring of epoxy prepolymers and primary amine groups attached on the surface of the AMS nanoparticles. The detailed characterizations of AMS/RS particles and their corresponding hybrid materials were performed and discussed in the following sections. The composition of hybrid materials is varied from 0 to 5 wt % of AMS nanoparticles and RS particles with respect to polymer content, and their mechanical and thermal properties were shown as summarized in Table I.

Spectroscopic studies of AMS nanoparticles

The as-prepared AMS nanoparticles were subsequently characterized by FTIR, ¹³C-NMR, and ²⁹Si-NMR spectroscopy, as shown in Figure 1. Figure

TABLE I
Relationship of the Composition of Epoxy-Silica Hybrid Materials with the *T_d*, *T_g*, *E'*, and Moisture Absorption Measured from TGA, DSC, DMA, and Water Uptake

Compound code	Epoxy resin component (g)			Feed composition (wt %)			Inorganic content found in product (wt %)	Thermal properties		Mechanical properties	Water uptake (wt %)
	TGTPM	BPA	T-403	Epoxy	AMS	RS		<i>T_d</i> (°C)	<i>T_g</i> (°C)		
Epoxy	0.5	0.5	0.68	100.0	0.0	0.0	0.443	339.8	33.7	920	8.94
AMS3	0.5	0.5	0.68	97.0	3.0	—	1.549	354.6	39.6	1360	8.21
AMS5	0.5	0.5	0.68	95.0	5.0	—	2.655	361.8	42.3	1520	8.02
RS3	0.5	0.5	0.68	97.0	—	3.0	1.991	342.8	34.4	1040	8.73
RS5	0.5	0.5	0.68	95.0	—	5.0	2.905	344.7	34.6	1220	8.59

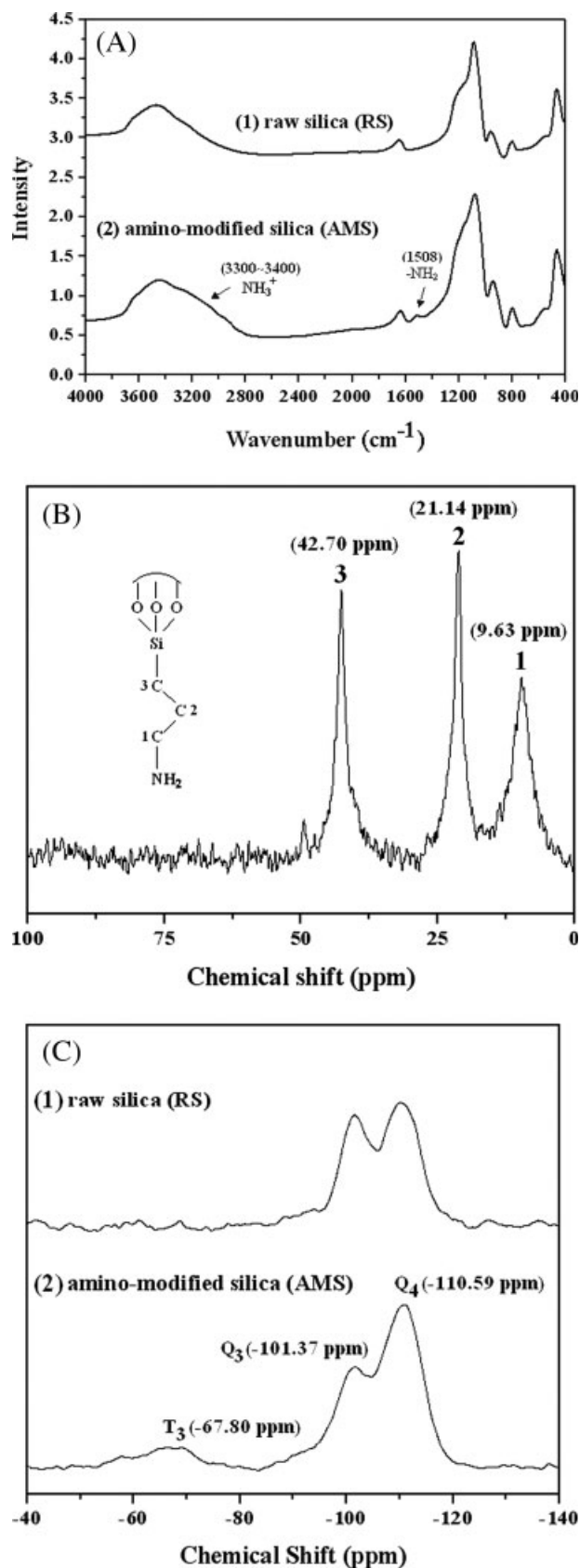


Figure 1 (A) FTIR absorption spectra of RS particles and AMS nanoparticles; (B) ¹³C CP-MAS NMR spectra of AMS nanoparticles; (C) ²⁹Si MAS NMR spectra of RS particles and AMS nanoparticles.

1(A) shows the representative FTIR spectroscopy of as-prepared RS particles and AMS nanoparticles. For example, the characteristic absorption band at 1508 and 3300–3400 cm⁻¹ were assigned to the symmetric bending vibration of —NH₂ and stretching vibration of NH₃⁺, respectively,^{22,23} indicating the existence of amine groups. The presence of organic groups in the materials after hydrolysis and condensation was confirmed using solid-state NMR spectroscopy. Figure 1(B) shows the solid-state ¹³C CP MAS NMR spectra of AMS nanoparticles, the AMS nanoparticles exhibit extra resonance peaks at chemical shifts $\delta = 9.6$, 21.1, and 42.7 ppm, respectively. These peaks are attributed to different carbon environments in the organosilane as denoted as C1, C2, and C3,^{22,23} indicating the incorporation of amine functional groups. Moreover, solid-state ²⁹Si MAS NMR provides information about the silicon environment. The ²⁹Si MAS NMR spectra of RS particles and AMS nanoparticles are presented in Figure 1(C). Two resonance peaks because of the silicon environments of Si(OSi)₄ (Q⁴, $\delta = -110.6$ ppm) and HOSi(OSi)₃ (Q³, $\delta = -101.4$ ppm) can be seen.^{22,23} In addition to these two peaks, the AMS nanoparticles display one more resonance peak at $\delta = -67.8$ ppm, assigned to R-Si(OSi)₃ (T³).^{22,23} The resonance peak (T³) appears owing to the modification of the surface of silica particles with aminopropyl group using APTES.

Morphology of epoxy-silica hybrid materials

The morphological studies for the dispersion capability of AMS nanoparticles and RS particles can be identified and compared by the observation of TEM. As shown in Figure 2, the TEM micrographs of AMS5 [Fig. 2(A)] at $\times 50$ k magnification exhibited a relatively well-dispersed silica nanoparticles with sizes ranging from ~ 20 to ~ 50 nm to the polymer matrix. However, the TEM image of RS5 obviously shows the aggregation of silica particle clusters, indicating a poor dispersion capability of silica particles embedded in epoxy matrix as compared to that of AMS nanoparticles, as shown in Figure 2(B).

Thermal properties

Figure 3(A) showed the typical TGA curves of the hybrid materials with AMS nanoparticles or RS particles, as measured under an air atmosphere. Three distinct stages of weight loss are appeared in the TGA curve for as-prepared low cross-linked epoxy resin starting at $\sim 80^\circ\text{C}$ and ending at $\sim 800^\circ\text{C}$, which might probably be correspond to the evaporation of moisture (i.e., 80–120°C), the structural decomposition of thermoplastic (i.e., 250–450°C) and thermosetting (i.e., 500–650°C) component of as-prepared materials. Typically, the thermal decomposition

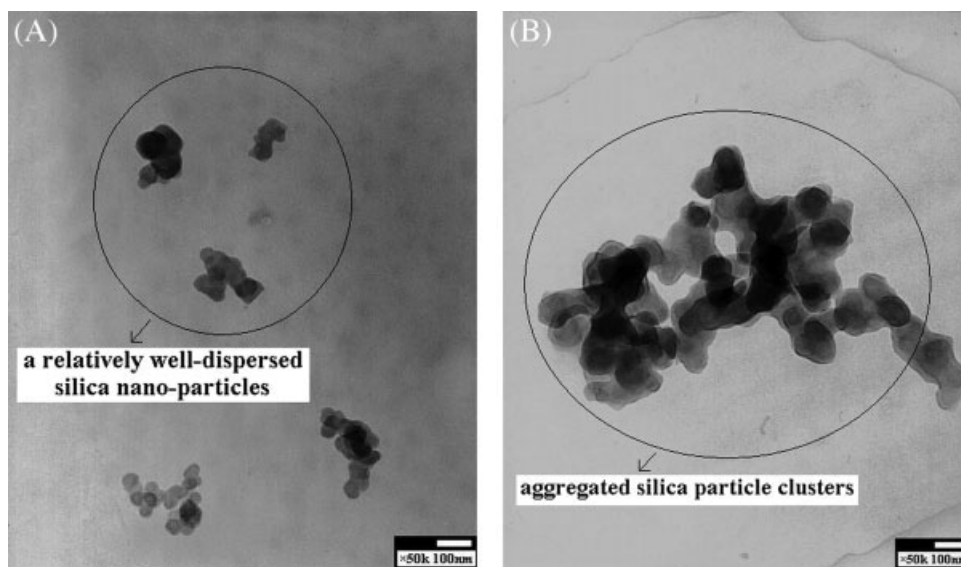


Figure 2 TEM micrographs of (A) AMS5 ($\times 50$ k); (B) RS5 ($\times 50$ k).

temperature (T_d) of the 10 wt % weight loss of the hybrid materials shifted to a higher temperature range accompanied with an increase of the silica content, which confirms the enhancement of thermal stability of hybrid materials, as shown in Figure 3 and Table I. Moreover, we also observed that the T_d of AMS5 was higher than that of RS5, which may probably be associated with the AMS materials showing higher interfacial contact area with epoxy matrix due to their better dispersion capability as compared to that of RS particles. The moisture absorption percentage of the hybrid materials with AMS nanoparticles or RS particles was given in Figure 3(B). It should be noted that the moisture absorption of hybrid materials reached a minimum value of 0.40 wt % in AMS5 as contrast to 1.30 wt % of pure epoxy, revealing an effective reduction in moisture absorption. This can be interpreted as follows: for the neat epoxy resin, the large amount of $-OH$ groups were formed as the ring-opening polymerization reactions of epoxy resin finished, leading to significant moisture absorption. After the incorporation of organophilic AMS nanoparticles, the reduced moisture absorption of hybrid materials could probably be resulted from the enhancement of hydrophobic characteristics of as-prepared hybrid materials. Moreover, well-dispersed silica nanoparticles in epoxy resin matrix showed lower moisture absorption than that of aggregated silica clusters. For example, AMS5 and RS5 exhibited the moisture absorption percentage of 0.40 and 0.96 wt %, respectively, as shown in Figure 3(B).

DSC traces of the pure epoxy and hybrid materials were shown in Figure 4 and Table I. The pure epoxy resin exhibited an endotherm at $33.7^\circ C$, corresponding to the T_g of epoxy resin. All the hybrid materials

showed an increased T_g compared to pure epoxy resin. This is tentatively attributed to the confinement of the hybrid polymer chains within the silica cage that prevent the segmental motions of the poly-

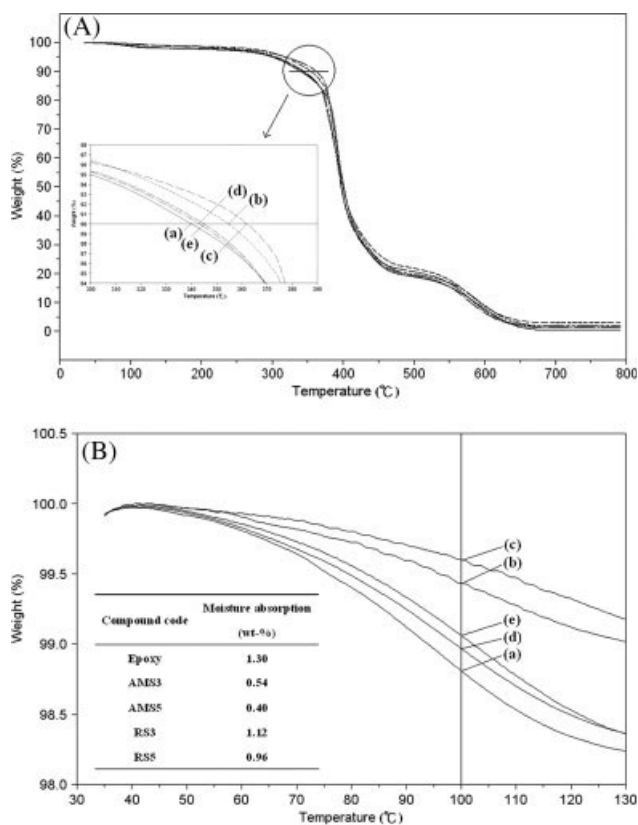


Figure 3 (A) TGA curves of (a) Epoxy, (b) AMS3, (c) AMS5, (d) RS3, and (e) RS5. 3; (B) Percentage (wt %) of moisture absorption for (a) Epoxy, (b) AMS3, (c) AMS5, (d) RS3, and (e) RS5.

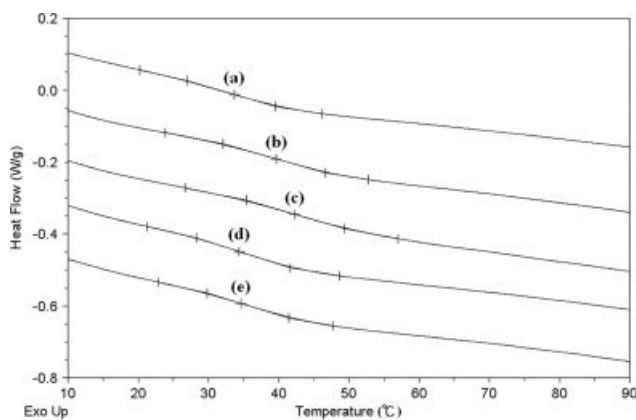


Figure 4 DSC curves of (a) Epoxy, (b) AMS3, (c) AMS5, (d) RS3, and (e) RS5.

mer chains. Moreover, we also found that the T_g of RS5 was lower than that of AMS5, which is probably also attributed to the lower interfacial contact area of RS5 between epoxy resin and RS particles, indicating that a better dispersion of silica particles in epoxy matrix led to a higher T_g of as-prepared composites.

Mechanical behavior

In this section, the mechanical behaviors of as-prepared hybrid materials were evaluated by DMA measurement. Dynamic mechanical tests at the frequency of 1 Hz were performed in order to measure the dynamic storage modulus curves (E') as a function of temperature. Figure 5 shows the representative E' curves for the hybrid materials in the temperature range of 30–100°C. The results are listed in Table I. It can be observed that the E' of the synthesized hybrid materials is higher than that of the pure epoxy throughout the temperature range studied. The AMS system was found to show a higher E'

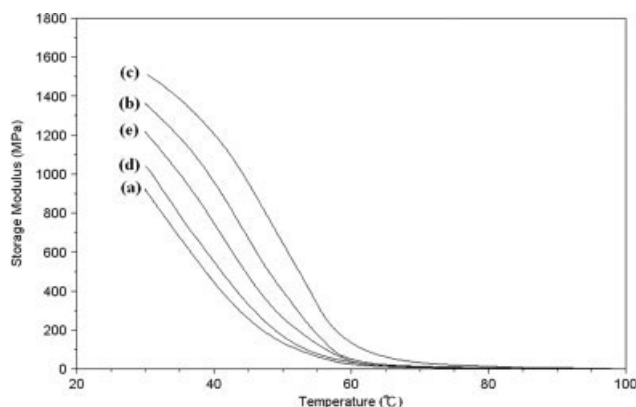


Figure 5 DMA curves of (a) Epoxy, (b) AMS3, (c) AMS5, (d) RS3, and (e) RS5.

than that of the RS system. This might probably be attributed to the strong interfacial interaction between the organic epoxy phase and the inorganic silica phase, with the nanosilica reinforcement sites.

Barrier properties

Polymer-silica hybrid materials can be used for packaging or storage tank applications in which the nano-dispersed silica reduced the permeability of gas in the polymer matrix. The presence of silica in nanocomposites increases the diffusion distance by creating a tortuous path which the diffusing species must be traversed. In this study, the free-standing film of pure epoxy and hybrid materials were prepared with film thickness of $\sim 170 \mu\text{m}$ and it is used for the evaluation of the molecular barrier and water uptake properties. The hybrid films loaded with low content of AMS nanoparticles (e.g., 3 wt %, AMS3) showed about 50.88% and 62.83% reduction in O_2 and N_2 permeability (in Fig. 6) than that of pure epoxy film, respectively. In addition, the barrier to water uptake for the pure epoxy and hybrid materials were evaluated by calculating the weight gains (wt %) after 24 h of uptake of water at room temperature. As listed in Table I, the water uptake was decreased by 8.17% from 8.94 wt % of epoxy to 8.21 wt % of AMS3. The significant reduction in gas permeability and water uptake may probably be associated with the barrier properties of the nanosilica effectively dispersed in the composites. Furthermore, AMS5 film showed an obvious decrease in the barrier of O_2 and N_2 molecule and the barrier to water uptake as compared to that of RS5 film, which may be resulted from effective uniform dispersion of the AMS nanoparticles than that of RS particles in the epoxy matrix. The conclusion is also consistent with our previous TEM observations.

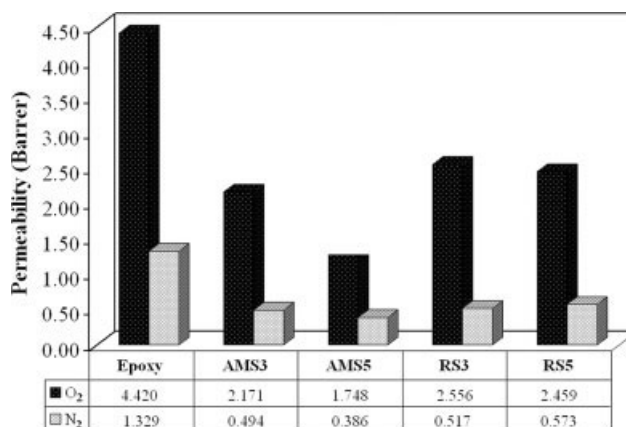


Figure 6 Gas permeability of O_2 and N_2 in the hybrid films.

CONCLUSIONS

In this article, epoxy hybrid materials filled with inorganic silica were successfully prepared. The hybrid materials consisted of epoxy resin matrix and well-dispersed AMS nanoparticles were found to exhibit an enhanced thermal, mechanical, and gas barrier properties as compared to the neat epoxy resin. Moreover, these hybrid materials were found to demonstrate significant effect in increasing the T_d , T_g , and E' and reducing moisture absorption and gas permeability than that of materials containing RS particles. It reflects that the hybrid materials have a higher interfacial contact area between organic and inorganic phases resulted from the better dispersion of AMS nanoparticles in epoxy resin as compared to that of aggregated RS particle clusters based on TEM studies. The better dispersion of AMS nanoparticles in epoxy matrices lead to enhanced thermal, mechanical properties and reduced moisture absorption, and gas permeability properties. The material may have a variety of industrial applications e.g., in packaging technology and as water repellent material.

References

1. Osman, M. A.; Atallah, A.; Muller, M.; Suter, U. W. *Polymer* 2001, 42, 6545.
2. Osman, M. A.; Mittal, V.; Lusti, H. R. *Macromol Rapid Commun* 2004, 25, 1145.
3. Ou, Y.; Yang, F.; Yu, Z. Z. *J Polym Sci Part B: Polym Phys* 1998, 36, 789.
4. Hackett, E.; Manias, E.; Ginneries, E. P. *Chem Mater* 2000, 12, 2161.
5. Liu, Y.-L.; Hsu, C.-Y.; Wei, W.-L.; Jeng, R.-J. *Polymer* 2003, 44, 5159.
6. Huang, C. J.; Fu, S. Y.; Zhang, Y. H.; Lauke, B.; Li, L. F.; Ye, L. *Cryogenics* 2005, 45, 450.
7. Qi, C.; Gao, H.; Yan, F.; Liu, W.; Bao, G.; Sun, X.; Chen, J.; Zheng, X. *J Appl Polym Sci* 2005, 97, 38.
8. Sun, Y.; Zhang, Z.; Wong, C. P. *Polymer* 2005, 46, 2297.
9. Preghenella, M.; Pegoretti, A.; Migliaresi, C. *Polymer* 2005, 46, 12065.
10. Zhang, H.; Zhang, Z.; Friedrich, K.; Eger, C. *Acta Mater* 2006, 54, 1833.
11. Jia, Q. M.; Zhang, M.; Xu, C. Z.; Chen, H. X. *Polym Adv Technol* 2006, 17, 168.
12. Wang, X.; Zhao, X.; Wang, M.; Shen, Z. *Polym Eng Sci* 2007, 47, 1156.
13. Zhang, W.; Blackburn, R. S.; Dehghani-Sanij A. A. *Scr Mater* 2007, 56, 581.
14. Lin, C. H.; Feng, C. C.; Hwang, T. Y. *Eur Polym J* 2007, 43, 725.
15. Rosso, P.; Ye, L. *Macromol Rapid Commun* 2007, 28, 121.
16. Sun, Y.; Zhang, Z.; Moon, K.; Wong, C. P. *J Polym Sci Part B: Polym Phys* 2004, 42, 3849.
17. Cao, Y. M.; Sun, J.; Yu, D. H. *J Appl Polym Sci* 2002, 83, 70.
18. Ash, B. J.; Schadler, L. S.; Siegel, R. V. *Mater Lett* 2002, 55, 83.
19. Xiong, M.; Gu, G.; You, B.; Wu, L. *J Appl Polym Sci* 2003, 90, 1923.
20. Yeh, J.-M.; Huang, H.-Y.; Cheng, C.-L.; Su, W.-F.; Yu, Y.-H. *Surf Coat Technol* 2006, 200, 2753.
21. Gupta, Y.; Hellgardt, K.; Wakeman, R. J. *J Membr Sci* 2006, 282, 60.
22. Chong, A. S. M.; Zhao, X. S. *J Phys Chem B* 2003, 107, 12650.
23. Wang, X.; Lin, K. S. K.; Chan, J. C. C.; Cheng, S. *J Phys Chem B* 2005, 109, 1763.